Available online at www.sciencedirect.com
ScienceDirect
Journal of Magnetic Resonance 186 (2007) 131–141
JMR Journal of Magnetic Resonance
www.elsevier.com/locate/jmr

Analyses, extensions and comparison of three experimental schemes for measuring ($^nJ_{CH} + D_{CH}$)-couplings at natural abundance

Kyryl Kobzar, Burkhard Luy *

Department Chemie, Organische Chemie II, Technische Universität München, Lichtenbergstrasse 4, D-85747 Garching, Germany

Received 15 November 2006; revised 5 February 2007
Available online 12 February 2007

Abstract

Three types of experiments for measuring $^nJ_{CH}$ heteronuclear long-range coupling constants are examined and extended with state-of-the-art pulse sequence building-blocks: The use of a HMBC with corresponding reference-HSQC for accurate coupling determination is combined with the constant time technique and the conversion of antiphase magnetization into ZQ/DQ-coherences; CPMG-based LR-CAHSQC and BIRD^{r,X}–HSQMBC experiments are examined in detail with respect to their coherence transfer properties; finally, the HSQC–TOCSY–IPAP experiment is introduced, a sequence derived from previously published α and β selective HSQC–TOCSYs using a different spin state selection technique and a recently developed ZQ-suppression method. The experiments are characterized with their advantages and disadvantages and compared using strychnine and menthol as standard molecules.

Keywords: HMBC; HSQMBC; BIRD; CPMG; HSQC–TOCSY; IPAP

1. Introduction

Long-range heteronuclear coupling constants play an important role in NMR-spectroscopic studies of small to medium-sized molecules. Especially $^3J_{CH}$ coupling constants follow the Karplus relation and build a more reliable tool for the determination of relative configurations as e.g. NOE connectivities, which often do not allow unambiguous conclusions [1–12].

But the measurement of long-range heteronuclear couplings is also of high interest for conformational studies: since the introduction of alignment media with sufficiently low induced anisotropy also for larger organic molecules [13–24], there is a demand for accurate measurement of long-range $^nJ_{CH}$ and the corresponding D_{CH} residual dipolar couplings (RDCs). In contrast to the $^3J_{CH}$ coupling determination in isotropic samples, magnitude *and* sign of the long-range couplings are of equal importance in partially aligned samples.

On our search for reliable experiments for detecting long-range heteronuclear RDCs, we examined a large number of pulse sequences. Out of the manifold of different techniques, the three experimental schemes discussed in this article are among the best available for measuring $^nJ_{CH}$ and the corresponding D_{CH} couplings. In this context, selected pulse sequences were also subject to modifications that resulted in improved spectral quality in our hands. Since all presented methods have been derived during recent years, it can also be understood as a kind of extension to the excellent survey provided by Marquez et al. [25], in which most of the previously published methods are already compared.

Three experiment types are explored in the following: The intensity and multiplet pattern based coupling measurement out of an HMBC with a corresponding reference HSQC [26], the pattern-based coupling extraction from CPMG-type transfer experiments [27–29], and the displacement based coupling determination from IPAP-type HSQC–TOCSY experiments [30,31].

* Corresponding author. Fax: +49 89 289 13210.
E-mail address: Burkhard.Luy@ch.tum.de (B. Luy).

1090-7807/$ - see front matter © 2007 Elsevier Inc. All rights reserved.
doi:10.1016/j.jmr.2007.02.005

2. HMBC and correlated reference HSQC

The idea of using a reference experiment for coupling extraction exists for quite some time now [32,33]. For heteronuclear long-range couplings usually proton-based reference experiments are recorded with identical phase distortions as the corresponding HMBC-type spectrum. This approach was recently extended significantly in the way that a given multiplet pattern can be fitted to its shape *and intensity simultaneously* by acquiring the corresponding reference HSQC with identical phase distortions due to ^{1}H, ^{1}H couplings [26]. Since signal intensities in HMBC experiments are proportional to $\sin \pi\, {}^nJ_{CH}T$ (T being the effective long-range transfer period), they can equally be used for coupling determination so long as the lineshape and intensity of a reference signal of an already determined coupling are known [26].

The originally published reference HSQC [26] involves two consecutive t_1-evolution periods and the resulting spectra in our hands contained considerable t_1-noise. It is also clear that intensities of the reference HSQC compared to the HMBC would vary significantly for molecules with non-negligible transverse relaxation. We therefore redesigned the reference experiment as shown in Fig. 1b: after the initial filter for one-bond-coupled coherences, $2I_xS_z$ terms are converted in heteronuclear ZQ/DQ-terms to avoid further coupling evolution. In this way, the reference experiment duration could be reduced to be identical to the corresponding HMBC experiment in Fig. 1a. As long as the relaxation of the ZQ/DQ-term does not significantly differ from the relaxation of the antiphase term $2I_xS_z$ present in the HMBC, the intensity and pattern based fitting procedure will be applicable.

A second modification to both experiments is the introduction of constant time (CT) evolution on carbon [34,35] for improved cross peak appearance (see Fig. 2). The main advantage is the elimination of the carbon chemical shift dependence of the measured multiplet lineshape, which helps to reduce errors in the subsequent fitting procedures.

In the sequence of Fig. 1a a first-order low-pass J-filter is incorporated which is sufficient to significantly reduce one-bond cross signals. The element is also found in a modified form (note the y-phase of the 90° pulse before the gradient) in the reference experiment in Fig. 1b to retain as many pulse sequence artifacts, like e.g. offset effects, as possible. Since higher-order low-pass J-filter elements complicate the situation for the reference experiment where we are interested specifically in one-bond correlations, we did not attempt their implementation.

We applied the pulse sequences to two widely used test samples, strychnine and menthol dissolved in $CDCl_3$. The overall quality of all spectra was good with no significant artifacts visible. The phase-sensitive processing of the data results in very complex multiplet patterns with significant dispersive contributions from homonuclear antiphase coherences. For the visualization of typical cross peaks and to give an impression of the accuracy of the fitting procedure, two characteristic signals from each CT-HMBC spectrum are shown in Fig. 3 with the corresponding lineshape and intensity fits for the best determined couplings and for small deviations of ±0.6 Hz. While the fit for large couplings is mainly determined by the lineshape, small couplings apparently profit significantly from the strong intensity dependence of their fit. This is, of course, due to the differences in transfer efficiency, which are proportional to $\sin \pi\, {}^nJ_{CH}T$ and are most sensitive for deviations of small $^nJ_{CH}$ couplings, for which the sine changes approximately

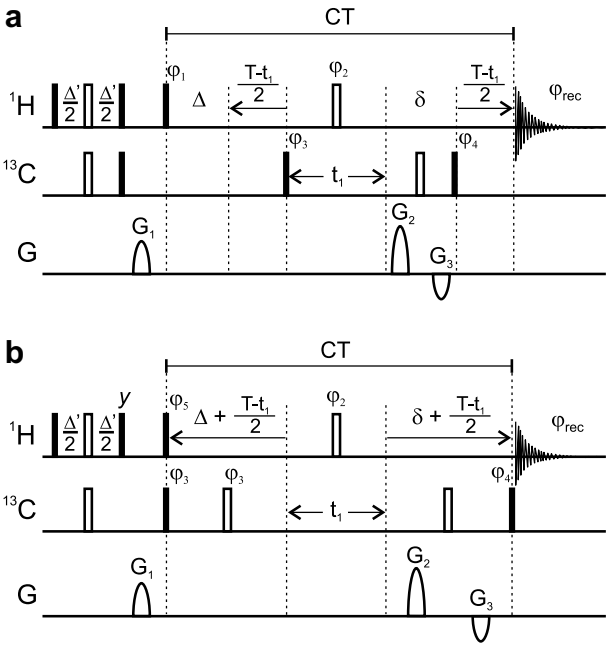

Fig. 1. Pulse sequences for the constant-time HMBC (a) and reference constant-time HSQC experiment (b). Narrow and thick bars represent 90° and 180° RF-pulses, respectively. Pulse phases are along x unless indicated otherwise. Phase cycles are: $\phi_1 = 4(x), 4(-x)$; $\phi_2 = 8(x), 8(y)$; $\phi_3 = -x, x$; $\phi_4 = x, x, -x, -x$; $\phi_5 = 4(y), 4(-y)$; $\phi_{rec} = x, -x, -x, x, -x, x, x, -x, -x, x, x, -x, x, -x, -x, x$. The long-range polarization transfer delay Δ is typically set to 62.5 ms, which corresponds to optimal transfer for a long-range heteronuclear coupling value of $^nJ_{CH} = 8$ Hz. The length of the constant time period T is set up according to the chosen spectral width in the indirect dimension and number of increments. Echo and antiecho selections were achieved using gradients. The gradient pulses were 1 ms long. The applied gradient strength ratios are: $G_1{:}G_2{:}G_3 = 33{:}50{:}-30$ for echo and $33{:}30{:}-50$ for antiecho. The carbon pulse phase ϕ_3 and ϕ_{rec} were incremented by π for every second t_1 increment to obtain States-TPPI-like data.

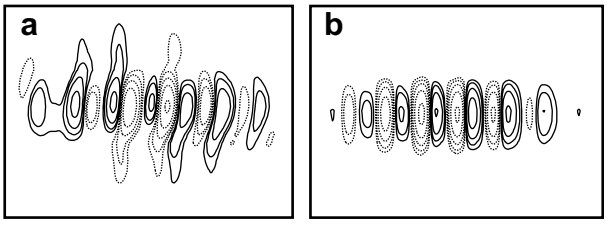

Fig. 2. A typical cross-peak acquired using a conventional HMBC sequence (a) and a constant-time HMBC (b). Dashed lines represent negative contour levels.

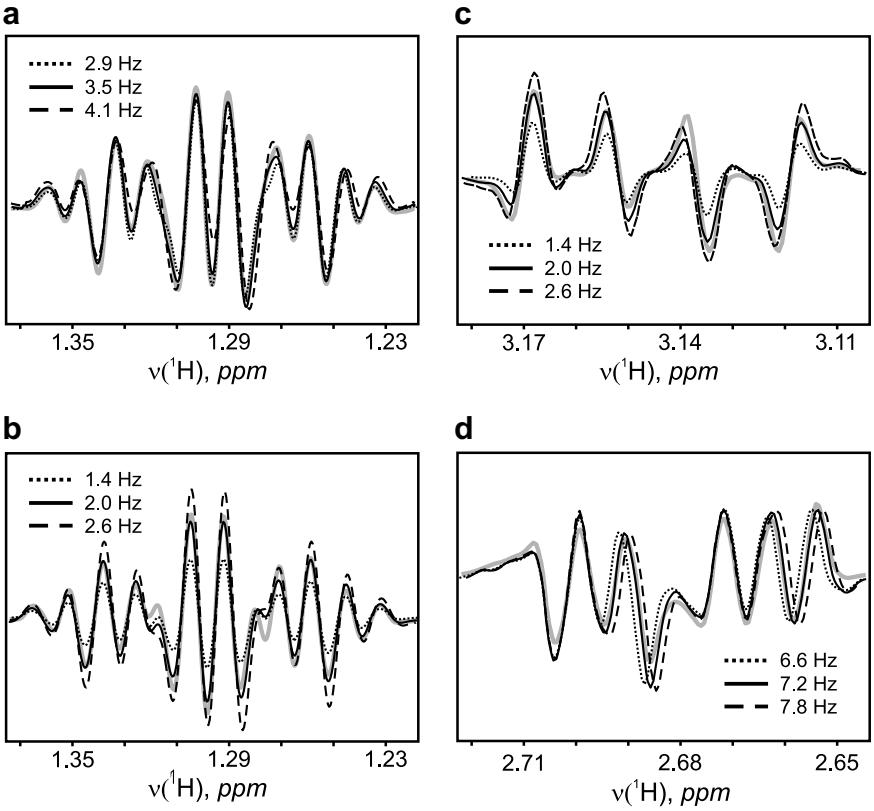

Fig. 3. Some fitting results for cross-peaks between H_1 and C_2 (a), and H_1 and C_3 (b) of menthol and between C_{12} and $H_{11,ax}$ and C_{12} and $H_{11,eq}$ (c and d) of strychnine in chloroform. The rows extracted from HMBC spectra are plotted grey and best fits are shown with solid lines. To assess the precision of measurement, two more traces are shown for each case, with 0.6 Hz larger (dashed line) and 0.6 Hz smaller (dotted line) trial couplings.

linearly. Larger $^nJ_{CH}$ couplings close to ideal transfer conditions, instead, show very similar signal intensities since the transfer efficiency describes a plateau in this case.

We found that coupling constants for the two test molecules could be determined quite reliably. The complex multiplet patterns with mixed absorptive and dispersive contributions help with the applicability of the fitting procedure but also make the acquisition of large data sets necessary. The coupling extraction procedure is not yet implemented in any available software, so that we had to write a minimization script for the fitting ourselves. The coupling determination from HMBC-type spectra is generally not sign-sensitive, as can also be seen in the original paper for the described procedure [26]. This fact strongly limits its use for the determination of long-range RDCs, where the sign contains valuable structural information.

3. CPMG-based experiments

Two kinds of CPMG-based, purely absorptive pulse sequences for measuring $^nJ_{CH}$ couplings can be found in the literature. The LR-CAHSQC [27] with a slight modification using composite pulses [28] and the socalled BIRD^{r,X}–CPMG–HSQMBC [29]. Sequences for both experiment types are shown in Fig. 4 with small additional changes: in the LR-CAHSQC version no suppression of heteronuclear one-bond coherences is applied since homonuclear isotropic mixing conditions distribute magnetization into the spin system anyway and in the BIRD^{r,X}–CPMG–HSQMBC the conventional BIRD^{r,X} filter element is replaced by a CAGEBIRD^{r,X} filter [36] for a more consequent use of the CPMG properties. For convenience, we will refer to the CAGEBIRD^{r,X}–CPMG–HSQMBC as the CBC-HSQMBC in the rest of the article.

CPMG-type periods for the transfer via small heteronuclear couplings were first applied in ^{1}H, ^{31}P-correlation experiments [37]. Due to the repeating inversion elements with typically an XY16 supercycle [38,39], TOCSY conditions are fulfilled for scalar couplings [40,27,41,37], leading to inphase transfer solely via undetectable ZQ-coherences. The absence of observable homonuclear antiphase coherences during the CPMG periods finally allows the phase sensitive detection of heteronuclear long-range correlations in pure absorption and with higher efficiency than previously published methods.

However, the approach comes with certain limitations, as for example the available bandwidth of the Hartmann–Hahn matching condition. The corresponding offset dependence of a typical XY16-expanded CPMG-sequence ($rf_{max} = 20$ kHz, $\Delta/2 = 100$ μs) for the homonuclear Hartmann–Hahn transfer $I_{1x} \rightarrow I_{2x}$ and the offset dependence describing the evolution of initial inphase coherences into

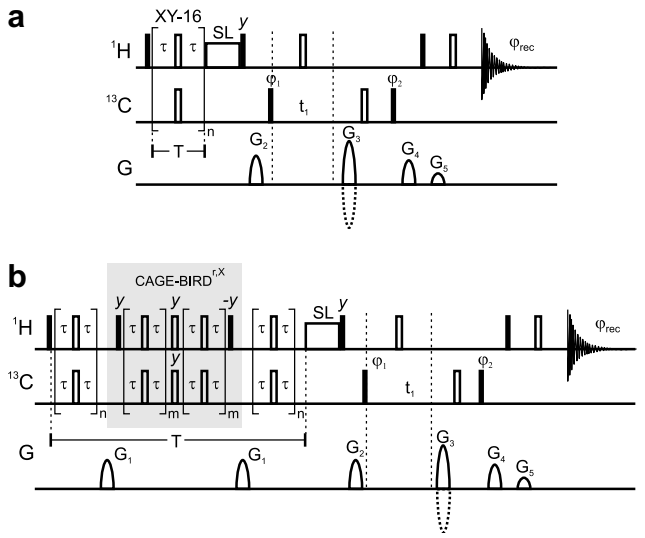

Fig. 4. Pulse sequences for the LR-CAHSQC (a) and CBC-HSQMBC (CAGEBIRD^{r,X}–CPMG–HSQMBC) experiment (b). Narrow and thick bars represent 90° and 180° RF-pulses, respectively. The unfilled rectangle represents a spin-lock pulse (1 ms). Pulse phases are along x unless indicated otherwise. Phase cycles are: $\phi_1 = x, -x$; $\phi_2 = x, x, -x, -x$; $\phi_{rec} = x, -x, -x, x$. The long-range polarization transfer delay T is typically set to 62.5 ms to roughly correspond to the usual transfer delay for the long-range coupling of ≈8 Hz. The CPMG-delay τ should be set equal or larger than 100 μs. The number of cycles in the CAGEBIRD element m corresponds to a single XY16 supercycle for the CPMG period. n is set to several XY16 supercycles in order to accommodate for the overall transfer duration T. Echo and antiecho selections were achieved using gradients G_3 and G_5. Gradient pulses have typical durations of 1 ms. Applied gradient strength ratios are: $G_1{:}G_2{:}G_3{:}G_4{:}G_5 = 33{:}50{:}\pm 80{:}41.7{:}20.1$. The carbon pulse phase ϕ_1 and the receiver phase ϕ_{rec} were incremented by π for every second t_1 increment to obtain States-TPPI-like data.

unwanted antiphase terms $I_{1x} + I_{2x} \rightarrow 2I_{1y}I_{2z}$ are given in Fig. 5a and b, respectively. Clearly visible is the correlation of efficient TOCSY inphase transfer (light area in Fig. 5a) with the absence of antiphase coherences (black area in Fig. 5b). The bandwidth for reasonable antiphase suppression can be estimated to ≈3000 Hz along the antidiagonal, which covers most protons on small to medium-sized spectrometers but does not allow coverage of the full proton chemical shift range on high fields. A similar offset dependence exists for the inversion of carbon nuclei. For typical ^{13}C rf-amplitudes of $rf_{max} = 12.5$ kHz and a CPMG-delay $\Delta/2 = 100$ μs the inversion bandwidth covers ≈11.8 kHz, which, of course, might be compensated to some extent by using appropriate composite pulses [43,28,42,44].

The main difference between the LR-CAHSQC and the CBC-HSQMBC is the transfer efficiency via long-range couplings to carbons directly attached to protons. For the LR-CAHSQC all nuclei of the corresponding spin system, i.e. the carbon and the coupled proton network, contribute to the coherence transfer. The most simple, non-trivial case is a three spin system consisting of a carbon, the directly bound proton and a remotely coupled proton, as shown in Fig. 6a and b. The coherence transfer function of the resulting ILL coupling topology (homonuclear isotropic mixing and heteronuclear longitudinal mixing conditions [45]) is mainly modulated by the homonuclear isotropic transfer and additional modulations are due to the large heteronuclear one-bond coupling. Depending on the combination of sign and size of the participating coupling constants and the transfer time chosen for the LR-CAHSQC, corresponding cross peaks can be inverted or even vanish (see the two cases shown in Fig. 6 for a typical $^3J_{CH}$ (a) and $^2J_{CH}$ coupling network (b)).

In the CBC-HSQMBC, instead, the effective coupling topology is reduced to 0L0, i.e. an effective heteronuclear two spin system, because the directly bound proton is decoupled by the CAGEBIRD^{r,X} element (Fig. 6c and d). This reduction of the effective spin system in the CBC-HSQMBC experiment compared to the LR-CAHSQC clearly gives an advantage concerning its applicability to compounds of unknown spin systems, since the effective spin systems are reduced and also unnecessary one-bond correlations are effectively removed.

Example cross peaks for coupling extraction from lineshape fitting using the LR-CAHSQC and CBC-HSQMBC are given in Fig. 7b–e. The corresponding reference

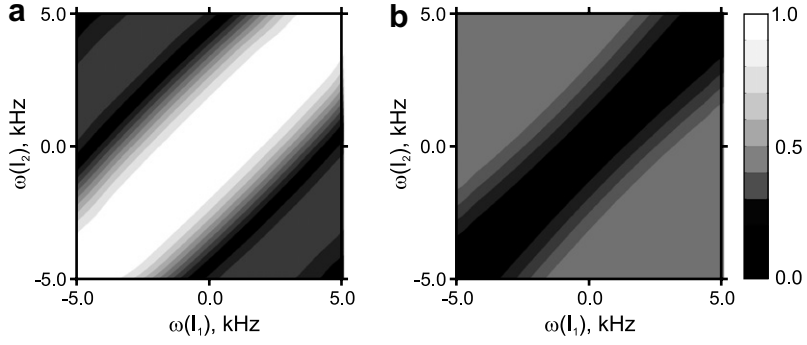

Fig. 5. Transfer properties of a CPMG pulse train as used in a pulse sequence of Fig. 4 with delay $\tau = 100$ μs and a hard inversion pulse applied at 20 kHz RF-power. Transfer is simulated for a homonuclear two-spin system with a $J = 12.63$ Hz isotropic coupling and optimal transfer length of $1/(2J) = 39.6$ ms. The offset dependence of the transfer efficiency are shown for typical TOCSY-transfer $I_{1x} \rightarrow I_{2x}$ (a) and the evolution of inphase into undesired antiphase terms $I_{1x} + I_{2x} \rightarrow 2I_{1y}I_{2z}$ (b). For the CPMG parameters chosen an active bandwidth for reasonable antiphase suppression can be derived to be approximately 3000 Hz along the antidiagonal.

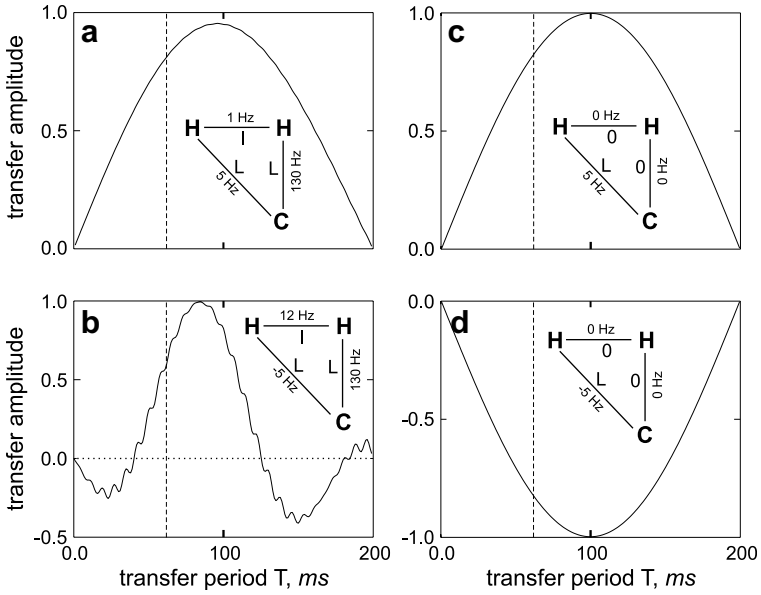

Fig. 6. The calculated efficiency of the transfer of in-phase proton magnetization to anti-phase carbon magnetization by a CPMG train for two typical constellations corresponding to $^{3}J_{CH}$ (a and c) and $^{2}J_{CH}$ (b and d) cases. Transfer functions for both the LR-CAHSQC corresponding to an effective ILL spin topology (a and b) and the CBC-HSQMBC with its effective 0L0 topology (c and d) are calculated. Vertical lines correspond to the mixing times used in actual experiments.

lineshapes can either be obtained from a conventional proton 1D-experiment or from slices of an HSQC. In the LR-CAHSQC the reference might also be taken from the corresponding one-bond correlation, if present. This case is shown in Fig. 7a.

For most signals the coupling measurement is straightforward and accuracy of the determined coupling is mainly limited by the signal-to-noise ratio of the corresponding cross peak. However, signals with broad multiplets and no characteristic, easily recognizable pattern pose a problem. In such cases, as for example demonstrated in Fig. 8 for the H_1–C_6 and H_2–C_1 cross peaks of menthol, lineshape fitting alone can result in a large uncertainty of up to several Hz.

A noteworthy effect concerning the pseudo-sign-sensitive determination of coupling constants should be mentioned: For a transfer time $T = 62.5$ ms the LR-CAHSQC provided all coupling constants of menthol with the correct relative sign (negative for $^{2}J_{CH}$, positive for $^{3}J_{CH}$ couplings) as demonstrated in Fig. 7b and c for two example cross peaks. This somewhat surprising result can be rationalized using the ILL topology of Fig. 6. Since the coherence transfer function is mainly influenced by the homonuclear coupling under isotropic mixing conditions, coherence transfer at $T = 62.5$ ms is achieved with identical sign for both $^{2}J_{CH}$ and $^{3}J_{CH}$ situations (Fig. 6a and b, respectively). The final evolution of the long-range antiphase coherence during acquisition is then sign-sensitive with $\sin \pi\, ^{n}J_{CH}$ (as seen in Fig. 7). Although the pseudo sign sensitivity in the coupling measurement might be present in many cases involving carbons with directly attached protons, coherence transfer properties are strongly influenced by the proton spin system and also depend strongly on the transfer time T used. It must be clearly stated that the LR-CAHSQC is generally *not* sign-sensitive. In the CBC-HSQMBC, multiplet patterns always have the same

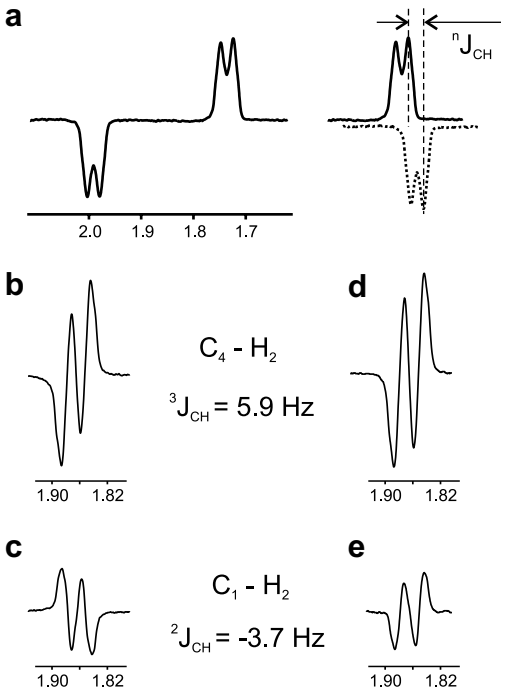

Fig. 7. Pattern-fitting procedure for coupling extraction out of both CPMG-based methods presented. (a) Reference signal taken from the H_2–C_2 cross peak of the LR-CAHSQC of menthol with the construction of the resulting antiphase multiplet sketched next to it. (b and c) example cross peaks taken from the LR-CAHSQC to indicate the pseudo-sign-sensitive measurement discussed in the text. (d and e) Identical cross peaks in the CBC-HSQMBC with no inversion of the multiplet-tilt.

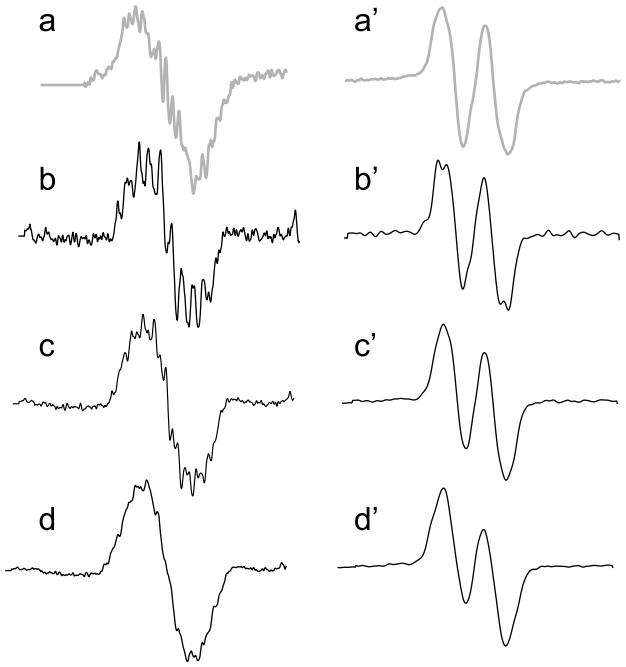

Fig. 8. Two examples of insufficient accuracy in coupling constant determination using the pattern-fitting approach. Slices through cross-peaks between H_1–C_6 (left, a) and H_2–C_1 (right, a′) of the LR-CAHSQC acquired on menthol in $CDCl_3$ are shown together with several pattern-fits for various couplings. Coupling constants as determined by the HSQC–TOCSY–IPAP approach (Fig. 9) are 3.4 Hz (a) and 1.8 Hz (a′). The trial peaks have been calculated for coupling constants of 3 Hz (b), 8 Hz (c), 15 Hz (d), and 2.0 Hz (b′), 4.2 Hz (c′), and 6.8 Hz (d′).

construction direction independent of the $^nJ_{CH}$ sign (cf. Fig. 7). Exceptions only occur in the case of negative ^{1}H, ^{1}H coherence transfer [46,47].

Both CPMG-based pulse sequences allow transfer via dipolar couplings [41]. However, for the combination of dipolar and scalar couplings CPMG-type transfer does not result in homonuclear isotropic mixing conditions, but rather in cylindrical mixing conditions [48,49] with inphase to antiphase evolution. Therefore spectra will contain dispersive elements and the advantage compared to conventional HMBC-type experiments is lost. In addition, ^{1}H, ^{1}H-RDCs typically provide broad multiplet patterns without characteristic elements and lineshape fitting alone does not lead to conclusive results, as was demonstrated in Fig. 8. Therefore the applicability of CPMG-based sequences seems to be limited to isotropic samples.

4. HSQC–TOCSY–IPAP

The first experiment published for sign-sensitive measurement of long-range $^nJ_{CH}$ couplings is the socalled HETLOC pulse sequence [31]. The E.COSY-type displacement in the resulting spectra contains information about the $^nJ_{CH}$ and $^1J_{CH}$ couplings of a specific carbon to its directly attached proton and the remote proton with the corresponding chemical shift of the cross peak in the directly acquired dimension. In addition to the size, the relative sign of long-range vs. one-bond couplings can be determined by the tilt of the E.COSY-pattern [50].

Many HSQC–TOCSY-type pulse sequences have been proposed based on the original principle with many additional modifications (see for example [51–53,31,54–57]). A significant improvement in terms of resolution was accomplished by the introduction of spin state selectivity [58,59,30,62], which separates multiplet components into two subspectra and therefore reduces the amount of signals in a single spectrum by a factor 2. The α and β-components in these experiments are selected either with spin state selective excitation [58] or via spin state selective coherence transfer [63,59]. These approaches work well so long as INEPT transfer delays are matched with the corresponding one-bond $^1J_{CH}$-couplings and the spin system is a simple heteronuclear two-spin system. Spin state selective coherence transfer does not work simultaneously for IS, I_2S, and I_3S groups unless multiple pulse sequences are used for matching HEHAHA conditions as in the SPITZE–HSQC [60]. The approach of acquiring inphase and antiphase spectra with subsequent addition/subtraction for obtaining the α/β-components does not rely on the conditions for spin state conservation during the transfer period and can be implemented easily for all spin systems of interest. A very nice package of pulse sequences for sensitivity enhanced HSQC-type spectra for this task was published recently [61]. However, since one of our aims in the present study is the potential application of pulse sequences to partially aligned samples with a wide distribution of $(^1J_{CH} + D_{CH})$ couplings, we were looking for an improved version for a spin state selective HSQC–TOCSY with clean α and β component spectra with as few as possible heteronuclear transfer periods to avoid errors from mismatched delays. The resulting pulse sequences based on the acquisition of inphase (HSQC–TOCSY–IP) and antiphase (HSQC–TOCSY–AP) spectra are shown in Fig. 9: Pure absorptive heteronuclear inphase or antiphase coherences are achieved by a single back-transfer INEPT step without sensitivity enhancement and by removing all undesired heteronuclear terms by phase cycled carbon pulses applied directly before the TOCSY mixing period. In addition, recently derived ZQ-suppression schemes [64] are introduced around the isotropic mixing multiple pulse sequence which considerably clean up the spectrum (Fig. 10).

The construction of spin state selective subspectra out of the HSQC–TOCSY–IPAP experiments is illustrated in Fig. 11 for simple cases. For typical isotropic samples with a narrow distribution of corresponding $^1J_{CH}$ coupling constants, INEPT transfer periods result in close to ideal performance and inphase and antiphase spectra are of equal intensity as long as aliphatic and aromatic regions are acquired separately. In such a case, spectra can be simply added or subtracted, respectively.

In cases where aliphatic and aromatic regions shall be covered in a single experiment or where partial alignment causes a wide distribution of $^1J_{CH} + D_{CH}$ couplings, IP and AP spectra will be clean in the HSQC–TOCSY–IPAP

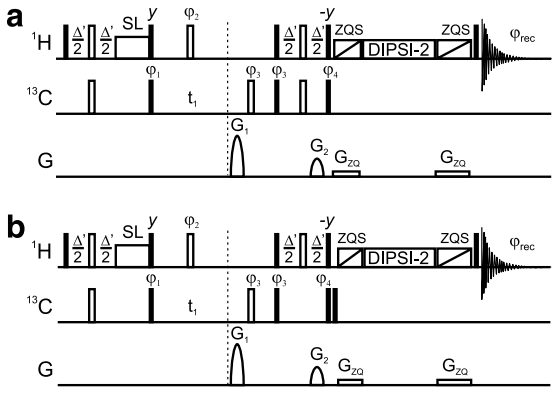

Fig. 9. Pulse sequences for the HSQC–TOCSY–IPAP approach, involving the inphase HSQC–TOCSY–IP (a) and anti-phase HSQC–TOCSY–AP (b) sequences. Narrow and thick bars represent 90° and 180° RF-pulses, respectively. Unfilled rectangles represent 1 ms spin-lock pulses. Pulse phases are along x unless indicated otherwise. Phase cycles are: $\phi_1 = x, -x$; $\phi_2 = x, x, -x, -x$; $\phi_3 = 4(x)\ 4(-x)$; $\phi_4 = x, -x$; $\phi_{rec} = x, -x, x, -x, x, -x, x, -x, x$. The INEPT-delay $\Delta = 1/(2^1J_{CH})$ is typically set to 3.846 ms corresponding to $^1J_{CH} = 130$ Hz. Open rectangles with oblique line represent adiabatic inversion pulses used in combination with gradient pulse G_{ZQ} as a filter to suppress unwanted zero-quantum coherences. The adiabatic pulses were chosen as smoothed Chirp pulses with 50 kHz sweep width over a duration of 30 and 50 ms, respectively. The G_{ZQ} gradient pulses are of corresponding durations and were calibrated using the detailed procedure provided online at http://www-keeler.ch.cam.ac.uk. Other gradient pulses are of 1 ms duration. Applied gradient strength ratios are: $G_1{:}G_2 = 64{:}16.1$. ϕ_1 was incremented according to the States-TPPI phase sensitive detection Scheme.

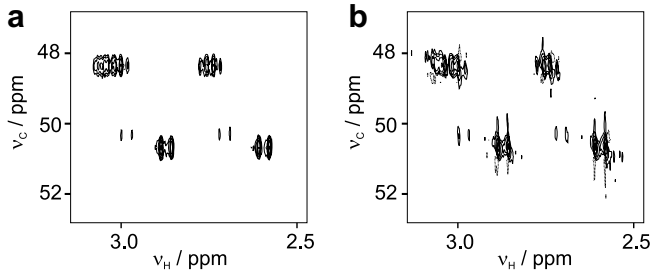

Fig. 10. Arbitrarily chosen region of the HSQC–TOCSY–IP spectra of strychnine acquired with (a) and without (b) ZQ-suppression scheme. Clearly the reduction of small artifacts is visible throughout the spectra.

experiments, but contain cross peaks of different intensities. This difference in intensities has to be corrected for each row by a simple procedure using standard functions for manipulation of 1D spectra as implemented in most processing programs like for example XWINNMR or TOPSPIN: First, identical rows have to be extracted from IP and AP spectra with corresponding diagonal cross peaks due to the direct $^1J_{CH}$ coupling. For the diagonal cross peaks with the large one-bond splitting, α and β components usually are well separated and clearly identifiable in the spectra and the intensity of IP and AP rows are easily adjusted until these diagonal components are of identical magnitude. Because the TOCSY transfer is identical for both the HSQC–TOCSY–IP and the HSQC–TOCSY–AP, it is sufficient to adjust the diagonal peak intensities (see also e.g. [65]). The intensity-adjusted rows can be saved and the corresponding sum and difference subspectra can directly be used for the $^nJ_{CH}$ coupling extraction by simply measuring the displacement of a certain cross peak in the two subspectra.

With the described procedure for coupling determination, the HSQC–TOCSY–IPAP approach can be applied identically to isotropic and partially aligned samples. The method is entirely sign-sensitive relative to the direct $^1J_{CH} + D_{CH}$ coupling which is usually of positive sign. In addition, spectra are very clean and far easier to interpret than other experiments examined. The major disadvantage of the approach is the limited number of couplings that can be extracted due to two limitations: Firstly, couplings can be measured only to carbons with directly attached protons, and secondly, not all remote protons might be reachable by the applied mixing scheme. Although TOCSY transfer provided excellent signal intensities for all potentially measurable long-range couplings for our two test molecules, transfer via DIPSI-2 and a single mixing time might not lead to sufficient signal intensities for all desired signals. In this case modifications to the mixing scheme can be tried like varying the mixing time, using tailored TOCSY sequences like for example the HNHA or COIN–TACSY [66,67], or even applying a totally different homonuclear mixing scheme like a NOESY period. For partially aligned samples, also the use of MOCCA-XY16 multiple pulse sequence might be considered which simultaneously allows efficient transfer also via homonuclear J_{HH} and D_{HH} couplings [40,41].

If resolution of the spectra is not sufficient, the pulse sequences of Fig. 9 might easily be extended to 3D versions with an additional ^{1}H evolution period before the homonuclear mixing scheme.

5. Experimental

All spectra were recorded on a Bruker Avance 500 spectrometer equipped with an 8 mm TXI probehead (a triple resonance room temperature probehead with a ^{13}C, ^{15}N outer and a ^{1}H-optimized inner coil) using a ≈500 mM menthol and a ≈100 mM strychnine sample dissolved in $CDCl_3$ in 5 mm NMR tubes.

The CT-HMBC and reference CT-HSQC (cf. Fig. 1) were acquired using a transfer delay $\Delta = 62.5$ ms with 8192 data points in 16 scans (strychnine) and 4096 in 4 scans (menthol), respectively, for 640 increments. LR-CAHSQC and BIRD^{r,X}–HSQMBC spectra were acquired with overall 35.7 ms long CPMG transfer periods with 100 μs delay τ (see Fig. 4) and 180° pulses applied with rf-amplitudes of 12.76 kHz on the proton channel and 7.16 kHz rf-amplitude on the carbon channel. 8192 data points in 16 scans (for strychnine) and 4096 data points in 4 scans (for menthol), respectively, were collected for each of the 640 increments in the indirect dimension.

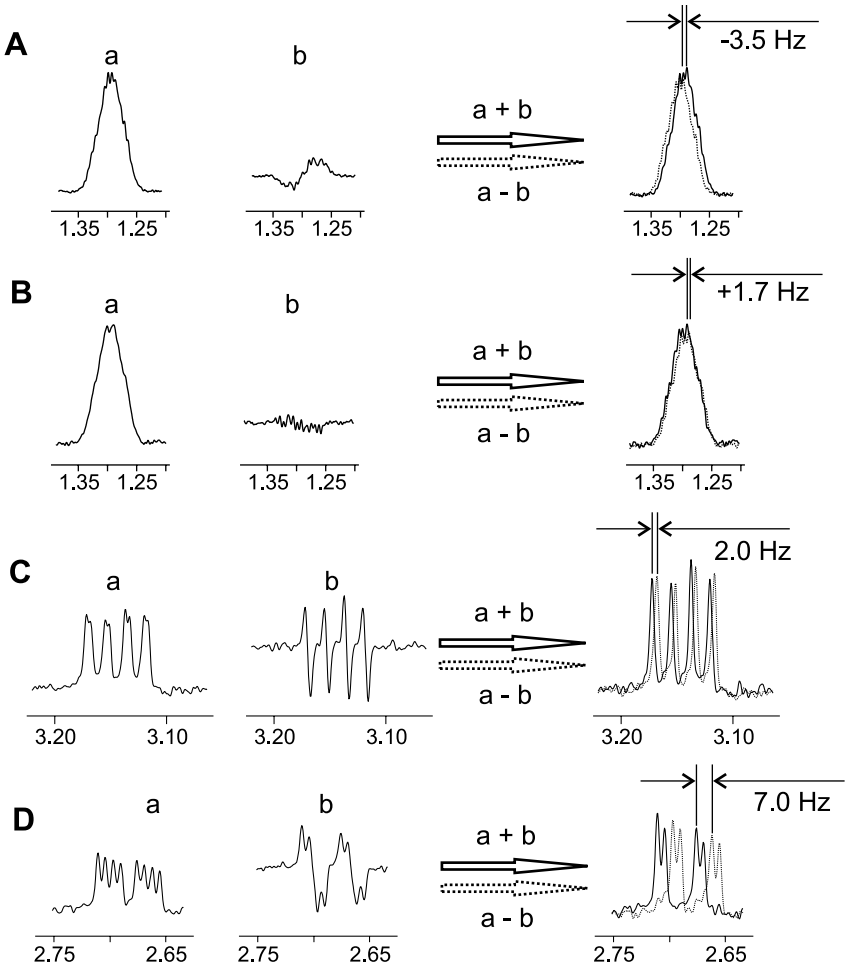

Fig. 11. The coupling measurement procedure of the HSQC–TOCSY–IPAP in its simplest form. Coupling determination is illustrated on the same example cross peaks used in Fig. 3: H_1–C_2 (A) and H_1–C_3 (B) of menthol and C_{12} to both H_{11} (C and D) of strychnine. The measurement is fully sign sensitive.

HSQC–TOCSY–IP and HSQC–TOCSY–AP spectra were acquired with 50 ms mixing time using the DIPSI-2 mixing sequence [68] applied at 6.38 kHz RF-power and the MOCCA-XY16 scheme as described in [40,41] with $\Delta/d = 2.2$, respectively. 8192 data points in 8 scans (strychnine) and 4096 data points in 2 scans (menthol), respectively, were collected for each of the 640 increments in the indirect dimension.

All spectra had an overall spectral width for strychnine of 10×120 ppm (folded signals did not overlap at the applied ^{13}C resolution) and 6×80 ppm for menthol and were processed by zero filling the data to 16384 points in the direct dimension and 1024 points in the indirect dimension. For apodization a 90°-shifted squared sine-bell weighting function was applied in both dimensions prior to Fourier-transformation.

6. Discussion

The precision of every coupling measurement strongly depends on the signal-to-noise ratio. All experiments discussed in this article provide very good sensitivity compared to other approaches for measuring long-range couplings. The CT-HMBC relies on the size of homonuclear *and* heteronuclear couplings evolving during acquisition of the corresponding antiphase terms. If these couplings are smaller than the linewidths, overlap of the multiplet components of opposite sign will significantly reduce the cross peak intensities. The same must be considered for heteronuclear couplings in the BIRD^{r,X}–HSQMBC and LR-CAHSQC, while homonuclear coherences (within limits) remain inphase during the CPMG transfer steps. The HSQC–TOCSY–IPAP results in inphase subspectra only so that reduction of signal intensities because of small involved couplings is not an issue in this case.

CPMG-based sequences and the HSQC–TOCSY–IPAP, on the other hand, depend on the homonuclear coherence transfer functions active in a particular spin system. Optimal sensitivity in this case can be achieved in principle by adjusting the TOCSY periods to the desired spin system, but in practice only empirically derived mixing times are applied once with more or less undefined intensities for the signals of interest. The sensitivity of the LR-CAHSQC in particular depends on the chosen mixing time (see Fig. 6)

due to the influence of the large heteronuclear one-bond coupling to the carbon of interest.

All experiments described here are designed for first order spectra. The presence of strong coupling or second order artifacts influences the extraction of coupling constants in several ways. For all intensity-based methods, ^{1}H, ^{1}H homonuclear coherence transfer via strong coupling contributions will lead to an exchange of ^{1}H, ^{13}C coherences and corresponding peak intensities are corrupted. Depending on the nature of the spin system this might lead to stronger or weaker signals. Since practically all homonuclear coupled spins have a slight second order contribution to their Hamiltonian, the measurement of couplings with a precision of less than ≈0.2 Hz in general is wishful thinking. For coupling extraction from pattern fitting like in the BIRD^{r,X}–HSQMBC or the CT-HMBC with the according reference-HSQC, the same caution has to be taken. Since the multiplet pattern is fit from a signal split by the corresponding heteronuclear one-bond coupling, second order effects on both multiplet components will be different. The effects will again be different for the signal of the $^{n}J_{CH}$ cross peaks of interest, since the chemical shift for each multiplet component is again shifted by a few Hz with slightly changed strong coupling contributions. The situation in the HSQC–TOCSY–IPAP is only better in the sense that second order effects are eventually easier recognizable due to differences in the peak shape of the α and β components. A measurement with higher accuracy is still not possible.

7. Conclusion

Three experimental schemes have been compared for measuring long-range heteronuclear scalar and residual dipolar couplings. Transfer properties of the HMBC with its correlated reference HSQC, the CBC-HSQMBC, and the LR-CAHSQC are dominated by the extended delays Δ and T, respectively, of an approximate duration of 60 ms for direct evolution of the long-range couplings of interest. The cross peak intensities in the case of the HSQC–TOCSY–IPAP sequences are determined by the homonuclear transfer, typically achieved via TOCSY of ≈50 ms duration. In all cases, acquisition parameters for the indirect dimension involve ^{13}C-evolution, which should be chosen in a way that ^{13}C-resolution is sufficient to avoid overlap as far as possible. Since quality of coupling constant extraction is directly influenced by the acquisition time of the FIDs, we recommend at least 8192 points in the directly recorded dimension.

For fast coupling measurement in isotropic samples and in cases where reliability and precision of couplings is not of utmost importance, as for example for configurational studies via $^{3}J_{CH}$ coupling constants in isotropic samples, the CBC-HSQMBC with pure absorptive inphase (t_1) and antiphase multiplets is most likely the experiment of choice. A single measurement provides all information needed and couplings can be extracted with reasonable effort.

For accurate coupling measurement with high reliability, we found that the HSQC–TOCSY–IPAP with pure absorptive multiplets with E.COSY-like displacements in the resulting α and β subspectra gave best results. It is the only one of the presented experiments providing the sign of the couplings relative to the large heteronuclear one-bond coupling. However, coupling measurement is limited to ^{1}H-attached carbons only. Therefore all remaining couplings have to be measured with additional methods, e.g. the presented CT-HMBC with its corresponding reference HSQC. Here, all cross peaks have absorptive inphase in the indirect dimension and mixed phases in the directly recorded dimension. Since lineshape and intensity can be fitted simultaneously, most reliable couplings are extracted. The missing sign-information must then be inferred from other data.

The signal-to-noise ratio is comparable for all examined pulse sequences with maybe the least average intensity for the LR-CAHSQC. For all other approaches signal intensities strongly depend on the couplings present in a particular spin system.

The aim of this article was the technical analysis and improvement of pulse sequences for measuring long-range scalar and residual dipolar couplings. The major complications arising for partially aligned samples today are more complex multiplet patterns and the need to measure the sign of the couplings. Both complicated multiplet patterns and couplings of varying sign are already abundantly available in isotropic samples that we used in our studies. Since there was no need in additional data for the technical analysis, we left out completely measurements on a number of aligned samples that we performed in the meantime. As expected, scalar and residual dipolar couplings can be measured in the way described in the article. Example data sets are available upon request from the authors.

A comparison with further experiments as e.g. the ones surveyed in [25] was not the aim of this article. Pulse programs for Bruker Avance consoles, example data sets and the matlab scripts used for the lineshape and intensity based coupling extraction out of HMBC data and the simulation of coherence transfer functions in an ILL spin topology will be made available at our website http://www.org.chemie.tu-muenchen.de/people/bulu.

Acknowledgment

B.L. thanks the Fonds der Chemischen Industrie and the DFG for financial support (Emmy Noether fellowship LU 835/1).

References

[1] M. Eberstadt, G. Gemmecker, D.F. Mierke, H. Kessler, Scalar coupling-constants—their analysis and their application for the elucidation of structures, Angew. Chem. Int. Ed. 34 (1995) 1671–1695.

[2] M. Eberstadt, D.F. Mierke, M. Köck, H. Kessler, Peptide conformation from coupling-constants—scalar couplings as restraints in MD simulations, Helv. Chim. Acta 75 (1992) 2583–2592.

[3] M. Köck, H. Kessler, D. Seebach, A. Thaler, Novel backbone conformation of cyclosporine A—the complex with lithium chloride, J. Am. Chem. Soc. 114 (1992) 2676–2686.
[4] N. Matsumori, D. Kaneno, M. Murata, H. Nakamura, K. Tachibana, Stereochemical determination of acyclic structures based on carbon-proton spin-coupling constants. A method of configuration analysis for natural products, J. Org. Chem. 64 (1999) 866–876.
[5] N. Matsumori, M. Murata, K. Tachibana, Conformational-analysis of natural-products using long-range carbon-proton coupling-constants—3-Dimensional structure of Okadaic acid in solution, Tetrahedron 51 (1995) 12229–12238.
[6] K.E. Milligan, B. Marquez, R.T. Williamson, M. Davies-Coleman, W.H. Gerwick, Two new malyngamides from a Madagascan Lyngbya majuscula, J. Nat. Prod. 63 (2000) 965–968.
[7] M. Murata, S. Matsuoka, N. Matsumori, G.K. Paul, K. Tachibana, Absolute configuration of amphidinol 3, the first complete structure determination from amphidinol homologues: application of a new configuration analysis based on carbon-hydrogen spin-coupling constants, J. Am. Chem. Soc. 121 (1999) 870–871.
[8] M. Murata, T. Yasumoto, The structure elucidation and biological activities of high molecular weight algal toxins: maitotoxin, prymnesins and zooxanthellatoxins, Nat. Prod. Rep. 17 (2000) 293–314.
[9] T. Rundlof, A. Kjellberg, C. Damberg, T. Nishida, G. Widmalm, Long-range proton-carbon coupling constants in conformational analysis of oligosaccharides, Magn. Reson. Chem. 36 (1998) 839–847.
[10] D. Seebach, S.Y. Ko, H. Kessler, M. Köck, M. Reggelin, P. Schmieder, M.D. Walkinshaw, J.J. Bolsterli, D. Bevec, Thiocyclosporins—preparation, solution and crystal-structure, and immunosuppressive activity, Helv. Chim. Acta 74 (1991) 1953–1990.
[11] M. Wu, T. Okino, L.M. Nogle, B.L. Marquez, R.T. Williamson, N. Sitachitta, F.W. Berman, T.F. Murray, K. McGough, R. Jacobs, K. Colsen, T. Asano, F. Yokokawa, T. Shioiri, W.H. Gerwick, Structure, synthesis, and biological properties of kalkitoxin, a novel neurotoxin from the marine cyanobacterium Lyngbya majuscula, J. Am. Chem. Soc. 122 (2000) 12041–12042.
[12] I. Tvaroska, F.R. Taravel, Carbon-proton coupling constants in the conformational analysis of sugar molecules, Adv. Carbohydr. Chem. Biochem. 51 (51) (1995) 15–61.
[13] B. Bendiak, Sensitive through-space dipolar correlations between nuclei of small organic molecules by partial alignment in a deuterated liquid solvent, J. Am. Chem. Soc. 124 (2002) 14862–14863.
[14] J.C. Freudenberger, S. Knör, K. Kobzar, D. Heckmann, T. Paululat, H. Kessler, B. Luy, Stretched poly(vinyl acetate) gels as NMR alignment media for the measurement of residual dipolar couplings in polar organic solvents, Angew. Chem. Int. Ed. 44 (2005) 423–426.
[15] P. Haberz, J. Farjon, C. Griesinger, A DMSO-compatible orienting medium: towards the investigation of the stereochemistry of natural products, Angew. Chem. Int. Ed. 44 (2005) 427–429.
[16] M.R. Hansen, L. Mueller, A. Pardi, Tunable alignment of macromolecules by filamentous phage yields dipolar coupling interactions, Nat. Struct. Biol. 5 (1998) 1065–1074.
[17] V.V. Klochkov, A.V. Klochkov, C.M. Thiele, S. Berger, A novel liquid crystalline system for partial alignment of polar organic molecules, J. Magn. Reson. 179 (2006) 58–63.
[18] B. Luy, K. Kobzar, H. Kessler, An easy and scalable method for the partial alignment of organic molecules for measuring residual dipolar couplings, Angew. Chem. Int. Ed. 43 (2004) 1092–1094.
[19] J.H. Prestegard, New techniques in structural NMR—anisotropic interactions, Nat. Struct. Biol. 5 (1998) 517–522.
[20] M. Rückert, G. Otting, Alignment of biological macromolecules in novel nonionic liquid crystalline media for NMR experiments, J. Am. Chem. Soc. 122 (2000) 7793–7797.
[21] H.J. Sass, G. Musco, S.J. Stahl, P.T. Wingfield, S. Grzesiek, Solution NMR of proteins within polyacrylamide gels: diffusional properties and residual alignment by mechanical stress or embedding of oriented purple membranes, J. Biomol. NMR 18 (2000) 303–309.
[22] C.M. Thiele, Simultaneous assignment of all diastereotopic protons in strychnine using RDCs: PELG as alignment medium for organic molecules, J. Org. Chem. 69 (2004) 7403–7413.
[23] N. Tjandra, A. Bax, Direct measurement of distances and angles in biomolecules by NMR in a dilute liquid crystalline medium, Science 278 (1997) 1111–1114.
[24] R. Tycko, F.J. Blanco, Y. Ishii, Alignment of biopolymers in strained gels: a new way to create detectable dipole–dipole couplings in high-resolution biomolecular NMR, J. Am. Chem. Soc. 122 (2000) 9340–9341.
[25] B.L. Marquez, W.H. Gerwick, R.T. Williamson, Survey of NMR experiments for the determination of $^{n}J_{CH}$ heteronuclear coupling constants in small molecules, Magn. Reson. Chem. 39 (2001) 499–530.
[26] L. Verdier, P. Sakhaii, M. Zweckstetter, C. Griesinger, Measurement of long range H,C couplings in natural products in orienting media: a tool for structure elucidation of natural products, J. Magn. Reson. 163 (2003) 353–359.
[27] H. Koskela, I. Kilpelainen, S. Heikkinen, LR-CAHSQC: an application of a Carr-Purcell-Meiboom-Gill-type sequence to heteronuclear multiple bond correlation spectroscopy, J. Magn. Reson. 164 (2003) 228–232.
[28] K.E. Köver, G. Batta, K. Fehér, Accurate measurement of long-range heteronuclear coupling constants from undistorted multiplets of an enhanced CPMG–HSQMBC experiment, J. Magn. Reson. 181 (2006) 89–97.
[29] V. Lacerda, G.V.J. da Silva, M.G. Constantino, C.F. Tormena, R.T. Williamson, B.L. Marquez, Long-range J(CH) heteronuclear coupling constants in cyclopentane derivatives, Magn. Reson. Chem. 44 (2006) 95–98.
[30] W. Kozminski, Simplified multiplet pattern HSQC–TOCSY experiment for accurate determination of long-range heteronuclear coupling constants, J. Magn. Reson. 137 (1999) 408–412.
[31] M. Kurz, P. Schmieder, H. Kessler, HETLOC, an efficient method for determining heteronuclear long-range couplings with Heteronuclei in natural abundance, Angew. Chem. Int. Ed. 30 (1991) 1329–1331.
[32] R.A.E. Edden, J. Keeler, Development of a method for the measurement of long-range C-13-H-1 coupling constants from HMBC spectra, J. Magn. Reson. 166 (2004) 53–68.
[33] J.J. Titman, D. Neuhaus, J. Keeler, Measurement of long-range heteronuclear coupling-constants, J. Magn. Reson. 85 (1989) 111–131.
[34] T.D.W. Claridge, I. Perez-Victoria, Enhanced C-13 resolution in semi-selective HMBC: a band-selective, constant-time HMBC for complex organic structure elucidation by NMR, Org. Biomol. Chem. 1 (2003) 3632–3634.
[35] K. Furihata, H. Seto, Constant time HMBC (CT-HMBC), a new HMBC technique useful for improving separation of cross peaks, Tetrahedron Lett. 39 (1998) 7337–7340.
[36] H. Koskela, I. Kilpelainen, S. Heikkinen, CAGEBIRD: improving the GBIRD filter with a CPMG sequence, J. Magn. Reson. 170 (2004) 121–126.
[37] B. Luy, J.P. Marino, H-1-P-31 CPMG-correlated experiments for the assignment of nucleic acids, J. Am. Chem. Soc. 123 (2001) 11306–11307.
[38] T. Gullion, D.B. Baker, M.S. Conradi, New, compensated Carr-Purcell sequences, J. Magn. Reson. 89 (1990) 479–484.
[39] M.J. Lizak, T. Gullion, M.S. Conradi, Measurement of like-spin dipole couplings, J. Magn. Reson. 91 (1991) 254–260.
[40] J. Furrer, F. Kramer, J.P. Marino, S.J. Glaser, B. Luy, Homonuclear Hartmann-Hahn transfer with reduced relaxation losses by use of the MOCCA-XY16 multiple pulse sequence, J. Magn. Reson. 166 (2004) 39–46.
[41] F. Kramer, W. Peti, C. Griesinger, S.J. Glaser, Optimized homonuclear Carr-Purcell-type dipolar mixing sequences, J. Magn. Reson. 149 (2001) 58–66.
[42] B. Luy, K. Kobzar, T.E. Skinner, N. Khaneja, S.J. Glaser, Construction of universal rotations from point-to-point transformations, J. Magn. Reson. 176 (2005) 179–186.

[43] K. Kobzar, T.E. Skinner, N. Khaneja, S.J. Glaser, B. Luy, Exploring the limits of broadband excitation and inversion pulses, J. Magn. Reson. 170 (2004) 236–243.
[44] M.A. Smith, H. Hu, A.J. Shaka, Improved broadband inversion performance for NMR in liquids, J. Magn. Reson. 151 (2001) 269–283.
[45] S.J. Glaser, J.J. Quant, Homonuclear and heteronuclear Hartmann-Hahn transfer in isotropic liquids, in: W.S. Warren (Ed.), Advances in Magnetic and Optical Resonance, 19, Academic Press, San Diego, 1996, pp. 59–252.
[46] B. Luy, S.J. Glaser, Negative polarization transfer between a spin 1/2 and a spin 1, Chem. Phys. Lett. 323 (2000) 377–381.
[47] M. Rance, Sign reversal of resonances via isotropic mixing in NMR-spectroscopy, Chem. Phys. Lett. 154 (1989) 242–247.
[48] B. Luy, S.J. Glaser, Superposition of scalar and residual dipolar couplings: analytical transfer functions for three spins 1/2 under cylindrical mixing conditions, J. Magn. Reson. 148 (2001) 169–181.
[49] D.M. Taylor, A. Ramamoorthy, Analysis of dipolar-coupling-mediated coherence transfer in a homonuclear two spin-1/2 solid-state system, J. Magn. Reson. 141 (1999) 18–28.
[50] C. Griesinger, O.W. Sørensen, R.R. Ernst, Correlation of connected transitions by two-dimensional NMR-spectroscopy, J. Chem. Phys. 85 (1986) 6837–6852.
[51] A. Bax, S. Subramanian, Sensitivity-enhanced two-dimensional heteronuclear shift correlation NMR-spectroscopy, J. Magn. Reson. 67 (1986) 565–569.
[52] A.S. Edison, W.M. Westler, J.L. Markley, Elucidation of amino-acid spin systems in proteins and determination of heteronuclear coupling-constants by carbon proton proton 3-dimensional NMR, J. Magn. Reson. 92 (1991) 434–438.
[53] J.R. Garbow, D.P. Weitekamp, A. Pines, Bilinear rotation decoupling of homonuclear scalar interactions, Chem. Phys. Lett. 93 (1982) 504–509.
[54] G. Otting, H. Senn, G. Wagner, K. Wüthrich, Editing of 2D H-1-NMR spectra using X half-filters—combined Use with residue-selective N-15 labeling of proteins, J. Magn. Reson. 70 (1986) 500–505.
[55] D. Uhrín, G. Batta, V.J. Hruby, P.N. Barlow, K.E. Köver, Sensitivity- and gradient-enhanced hetero ω_1 half-filtered TOCSY experiment for measuring long-range coupling constants, J. Magn. Reson. 130 (1998) 155–161.
[56] U. Wollborn, D. Leibfritz, Measurements of heteronuclear long-range coupling-constants from inverse homonuclear-2D NMR-spectra, J. Magn. Reson. 98 (1992) 142–146.
[57] G.Z. Xu, J.S. Evans, Determination of long-range J(XH) couplings using "excitation-sculpting" gradient-enhanced heteronuclear correlation experiments, J. Magn. Reson. Ser. A 123 (1996) 105–110.
[58] A. Meissner, J.O. Duus, O.W. Sørensen, Integration of spin-state selective excitation into 2D NMR correlation experiments with heteronuclear ZQ/DQ π rotations for $^1J_{XH}$-resolved E.COSY-type measurement of heteronuclear coupling constants in proteins, J. Biomol. NMR 10 (1997) 89–94.
[59] M.D. Sørensen, A. Meissner, O.W. Sørensen, Spin-state-selective coherence transfer via intermediate states of two-spin coherence in IS spin systems. Application to E.COSY-type measurement of J coupling constants, J. Biomol. NMR 10 (1997) 181–186.
[60] T. Carlomagno, W. Peti, C. Griesinger, A new method for the simultaneous measurement of magnitude and sign of $^1D_{CH}$ and $^1D_{HH}$ dipolar couplings in methylene groups, J. Biomol. NMR 17 (2000) 99–109.
[61] P. Nolis, J.F. Espinosa, T. Parella, Optimum spin-state selection for all multiplicities in the acquisition dimension of the HSQC experiment, J. Magn. Reson. 180 (2006) 39–50.
[62] P. Nolis, T. Parella, Spin-edited 2D HSQC–TOCSY experiments for the measurement of homonuclear and heteronuclear coupling constants: Application to carbohydrates and peptides, J. Magn. Reson. 176 (2005) 15–26.
[63] A. Ross, M. Czisch, T.A. Holak, Selection of simultaneous coherence pathways with gradient pulses, J. Magn. Reson. Ser. A 118 (1996) 221–226.
[64] M.J. Thrippleton, J. Keeler, Elimination of zero-quantum interference in two-dimensional NMR spectra, Angew. Chem. Int. Ed. 42 (2003) 3938–3941.
[65] B. Luy, Spin state selectivity and heteronuclear Hartmann-Hahn transfer, J. Magn. Reson. 168 (2004) 210–216.
[66] T. Carlomagno, T. Prasch, S.J. Glaser, COIN TACSY, a novel approach to tailored correlation spectroscopy, J. Magn. Reson. 149 (2001) 52–57.
[67] J. Quant, T. Prasch, S. Ihringer, S.J. Glaser, Tailored correlation spectroscopy for the enhancement of fingerprint cross peaks in peptides and proteins, J. Magn. Reson. Ser. B 106 (1995) 116–121.
[68] A.J. Shaka, C.J. Lee, A. Pines, Iterative schemes for bilinear operators; application to spin decoupling, J. Magn. Reson. 77 (1988) 274–293.